

Challenge for Detecting the Interface between Electrode and Electrolyte with β -NMR

Jun SUGIYAMA¹, Izumi UMEGAKI¹, Susumu SHIRAKI², Taro HITOSUGI^{2,3},
Ryan M. L. McFADDEN^{4,5}, Dongsheng WANG⁶, Victoria KARNER^{4,5}, Gerald D. MORRIS⁷,
W. Andrew MACFARLANE^{4,5,7}, and Robert F. KIEFL^{5,6,7}

¹Toyota Central Research & Development Labs., Inc. 41-1 Yokomichi, Nagakute, Aichi 480-1192, Japan,

²Advanced Institute for Materials Research, Tohoku University, Sendai, Miyagi 980-8577, Japan,

³School of Materials and Chemical Technology, Tokyo Institute of Technology, Tokyo 152-8552, Japan,

⁴Department of Chemistry, University of British Columbia, Vancouver, BC, V6T 1Z1, Canada

⁵Quantum Matter Institute, University of British Columbia, Vancouver, British Columbia, BC, V6T 1Z4, Canada

⁶Department of Physics & Astronomy, University of British Columbia, Vancouver, BC, V6T 1Z1, Canada

⁷TRIUMF, 4004 Wesbrook Mall, Vancouver, BC, V6T 2A3, Canada

E-mail: e0589@mosk.tytlabs.co.jp

(Received June 14, 2017)

It is widely believed that a space-charge layer (SCL) exists at the vicinity of a boundary between a solid electrolyte layer and electrode layer in an all solid-state Li-ion battery due to the difference of their chemical potentials, although there are no direct experimental evidences. Here, the Li concentration is predicted to decrease drastically in the SCL. In order to clarify whether SCL exists or not, we have attempted to measure the ^8Li β -NMR spectrum for a multilayer sample, MgO(50 nm)/Li₃PO₄(70 nm)/LiCoO₂(200 nm) as a function of implanted energy of ^8Li . The resonance spectrum was fitted by a combination of two Lorentzians and one background signal. Furthermore, the line width of the resonance signal from the Li₃PO₄ layer is found to become broad towards the boundary with the LiCoO₂ layer. This is consistent with the presence of an SCL.

KEYWORDS: interface, solid electrolyte, Li concentration, β -NMR

1. Introduction

In order to improve safety and volumetric charge density of the current Li-ion batteries, an all solid-state battery, which consists of a solid cathode, solid anode, and solid electrolyte, has been heavily investigated. The most significant issue to overcome for realizing an all solid-state battery was how to control the interface layer, which is newly formed during a charge and discharge reaction, between electrode and electrolyte. In fact, based on electrochemical analyses and ex-situ compositional analyses, such a layer, i.e. a solid-electrolyte interface (SEI), is known to exist in conventional Li-ion batteries using a liquid electrolyte [1]. Moreover, a similar layer is likely formed even for an all solid-state battery [2].

Very recently, the second issue was predicted by first principles calculations [3]. That is, the formation of a space-charge layer (SCL) at the interface between cathode and electrolyte due to the difference of their chemical potentials. In other words, Li vacancies are spontaneously formed particularly in the electrolyte layer at the vicinity of interface. Furthermore, the vacancy concentration

is expected to decrease with the distance from the interface and finally become negligibly small. Such an SCL naturally increases the interfacial resistance, leading to the decrease in both the working voltage and response time to rapid charge/discharge. For the worst case, an all solid-state battery would not work due to the SCL.

At present, there are neither experimental information on the thickness of SCL nor direct evidence its existence. However, it is empirically believed that SCL exists at the interface, because the oxide buffer layer interposed between the LiCoO_2 cathode and the sulfide electrolyte significantly reduces the interfacial resistance [4]. In addition, electric potential distribution measurements in an all solid-state battery ($\text{LiCoO}_2/\text{Li}_{1+x+y}\text{Al}_y\text{Ti}_2\text{ySi}_x\text{P}_{3x}\text{O}_{12}/\text{Li}$) showed a potential gradient in the electrolyte layer within approximately 1000 nm of the interface [5]. Nevertheless, more reliable or direct evidence of the SCL is required to further improve the interface in an all solid-state battery.

In order to observe the SCL, we definitely need a nondestructive technique with a good depth resolution, since the attempt to fabricate the samples for cross-section-view observations alters and/or destroys the potential gradient at the interface. Here, Li-NMR is one of the powerful tools to observe the Li-distribution in solids, but Li-NMR unfortunately lacks a depth resolution. We, therefore, attempted to use a β -NMR technique with a polarized ^8Li beam of TRIUMF, because the range of $^8\text{Li}^+$ is tunable by adjusting the implantation energy of $^8\text{Li}^+$ (E_{imp}). In the SCL, the resonance line is expected to become very broad due to the decrease in the Li concentration. Thus, we have mainly measured the resonance spectrum as a function of E_{imp} .

2. Experimental

A multilayers sample, $\text{MgO}(50 \text{ nm})/\text{Li}_3\text{PO}_4(70 \text{ nm})/\text{LiCoO}_2(200 \text{ nm})$, was prepared on a sapphire substrate by laser ablation at Tohoku University [see Fig. 1(a)]. The details of the thin-film-deposition conditions are published elsewhere [6, 7]. Here, the MgO layer is used for protecting Li_3PO_4 from air, because Li_3PO_4 is highly reactive with water.

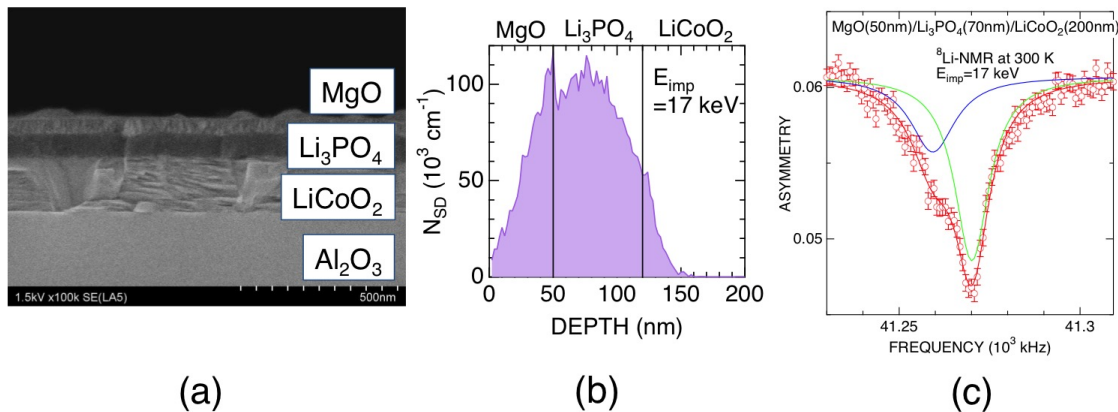


Fig. 1. (a) Cross section SEM observation view of the $\text{MgO}/\text{Li}_3\text{PO}_4/\text{LiCoO}_2$ multilayers sample grown on a sapphire substrate, (b) The normalized stopping distribution (N_{SD}) of ^8Li with $E_{\text{imp}} = 17 \text{ keV}$ in the multilayers sample, and (c) The ^8Li -NMR spectrum measured at 300 K with $E_{\text{imp}} = 17 \text{ keV}$ and $H = 6.55 \text{ T}$. In (b), the distribution was simulated by a computer program SRIM [9]. In (c), a blue solid line corresponds to the signal from LiCoO_2 , while a green line from MgO and Li_3PO_4 .

The β -NMR spectra were measured using the ^8Li beam produced at the Isotope Separator and Accelerator (ISAC) at TRIUMF in Canada. The nuclear spin is polarized using a collinear optical pumping method, producing a spin polarized $^8\text{Li}^+$ beam with about 70% polarization. The implanted

beam energy ($E_{\text{Li}}^{\text{imp}}$) was changed from 6 keV to 20 keV, for which the ^8Li stops at an average depth from about 30 nm to 130 nm. The details of setup and experimental procedure of β -NMR are described elsewhere [8, 10–13].

3. Results and Discussion

Figure 1(c) shows the resonance line in the multilayers sample recorded at 300 K with $E_{\text{imp}} = 17$ keV and $H = 6.55$ T. Here, H is applied parallel to the initial ^8Li spin polarization. The resonance line is fitted by a combination of the frequency independent baseline determined by the spin-lattice relaxation rate ($1/T_1$) [14], and two Lorentzians. Although the SRIM simulation [9] suggests the contribution from the three layers to the resonance spectrum [Fig. 1(b)], it is challenging to fit with more than two Lorentzians, presumably because the resonance frequency (f_r) of MgO is very close to that of Li_3PO_4 . It should be much narrower than in the Li_3PO_4 layer, given the lack of nuclear moments.

Figure 2 shows the resonance parameters as a function of E_{imp} at 300 K, — namely, the two amplitudes ($A1$, $A2$), resonance frequencies (f_{r1} , f_{r2}), and full width at half maximum (FWHM1, FWHM2) of the Lorentzian signals, together with a baseline. According to the temperature dependence of $1/T_1$ in Li_3PO_4 , FWHM of the Li_3PO_4 layer is motional narrowed at 300 K due to Li-diffusion. In addition, FWHM of the LiCoO_2 layer ranges around 5.8 kHz due to the appearance of localized moments [15, 16].

Therefore, we attribute the $A1$ signal at $E_{\text{imp}} \geq \sim 16$ keV to ^8Li stopped in the LiCoO_2 layer. Furthermore, f_{r2} and FWHM2 are almost independent of E_{imp} , particularly in the E_{imp} range below about 16 keV. Meanwhile, $A2$ decreases roughly monotonically with E_{imp} up to 15 keV. This suggests the $A2$ signal at $E_{\text{imp}} \leq 15$ keV corresponds to the signal from the MgO layer.

As a result, the $A1$ signal at $10 \text{ keV} \leq E_{\text{imp}} \leq 15$ keV and the $A2$ signal at $E_{\text{imp}} \geq 15$ keV are assigned as the signal mainly from the Li_3PO_4 layer. In this E_{imp} range, the FWHM1-vs.- E_{imp} curve is found to show a local maximum at $E_{\text{imp}} = 13$ keV at 300 K. This probably corresponds to the SLC, as expected.

Since the baseline is known to be decreased with increasing $1/T_1$ [14], Fig. 2(d) means the increase in $1/T_1$ with E_{imp} up to 15 keV. Then, $1/T_1$ is likely to slowly decrease, or eventually level off to a constant value, with further increasing E_{imp} in the LiCoO_2 layer. This would also suggest that

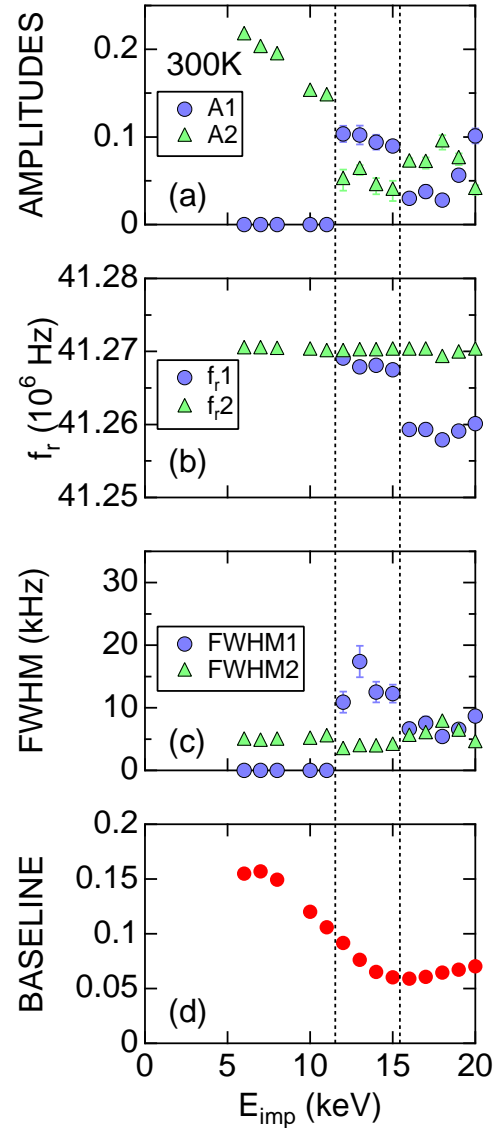


Fig. 2. The E_{imp} dependences of the (a) amplitudes (A), (b) resonance frequencies (f_r), (c) full width at half maximum (FWHM), and (d) baseline of the ^8Li β -NMR at 300 K. The data were obtained by fitting the resonance spectrum with two Lorentzians and one E_{imp} -independent baseline signal [see Fig. 1(b)]. Broken lines roughly represent the boundaries.

$1/T_1$ increases in the SLC probably due to the decrease in the Li content towards the boundary to the LiCoO_2 layer.

However, in order to confirm the existence of the SLC, further information on the Li distribution, via β -NMR, is required, particularly for the data at low temperatures. This is because Li^+ ions are naturally immobile at low temperatures, and as a result, the distribution of Li in the SLC is expected to strongly depend on temperature.

4. Acknowledgements

We thank the staff of TRIUMF for help with the β -NMR experiments and Mr. J. Seki of Toyota CRDL for SEM observation. This work was supported by the Ministry of Education, Culture, Sports, Science and Technology (MEXT) of Japan, KAKENHI Grant No. JP23108003 and Japan Society for the Promotion Science (JSPS) KAKENHI Grant No. JP26286084.

References

- [1] K. Xu, Chem. Rev. **104**, 4303 (2004).
- [2] R. Kanno, private communication (2012).
- [3] J. Haruyama, K. Sodeyama, L. Han, K. Takada, and Y. Tateyama, Chem. Mater. **26**, 4248 (2014).
- [4] N. Ohta, K. Takada, L. Zhang, R. Ma, M. Osada, and T. Sasaki, Adv. Mater. **18**, 2266 (2006).
- [5] K. Yamamoto, Y. Iriyama, T. Asaka, T. Hirayama, H. Fujita, C. A. J. Fisher, K. Nonaka, Y. Sugita, and Z. Ogumi, Angew. Chem. Int. Ed. **49**, 4414 (2010).
- [6] S. Shiraki, H. Oki, Y. Takagi, T. Suzuki, A. Kumatani, R. Shimizu, M. Haruta, T. Ohsawa, Y. Sato, Y. Ikuhara, and T. Hitosugi, J. Power Sources **267**, 881 (2014).
- [7] M. Haruta, S. Shiraki, T. Suzuki, A. Kumatani, T. Ohsawa, Y. Takagi, R. Shimizu, and T. Hitosugi, Nano Lett. **15**, 1498 (2015).
- [8] W. MacFarlane, Solid State Nuclear Magnetic Resonance **68-69**, 1 (2015).
- [9] <http://www.srim.org/>
- [10] Z. Salman, E. P. Reynard, W. A. MacFarlane, K. H. Chow, J. Chakhalian, S. R. Kreitzman, S. Daviel, C. D. P. Levy, R. Poutissou, and R. F. Kiefl, Phys. Rev. B **70**, 104404 (2004).
- [11] G. D. Morris, W. A. MacFarlane, K. H. Chow, Z. Salman, D. J. Arseneau, S. Daviel, A. Hatakeyama, S. R. Kreitzman, C. D. P. Levy, R. Poutissou, et al., Phys. Rev. Lett. **93**, 157601 (2004).
- [12] Z. Salman, R. F. Kiefl, K. H. Chow, M. D. Hossain, T. A. Keeler, S. R. Kreitzman, C. D. P. Levy, R. I. Miller, T. J. Parolin, M. R. Pearson, et al., Phys. Rev. Lett. **96**, 147601 (2006).
- [13] G. D. Morris, Hyperfine Interact. **225**, 173 (2014).
- [14] M. D. Hossain, H. Saadaoui, T. J. Parolin, Q. Song, D. Wang, M. Smadella, K. H. Chow, M. Egilmez, I. Fan, R. F. Kiefl, S. R. Kreitzman, C. D. P. Levy, G. D. Morris, M. R. Pearson, Z. Salman, and W. A. MacFarlane, Physica B **404**, 914 (2009).
- [15] K. Mukai, Y. Aoki, D. Andreica, A. Amato, I. Watanabe, S. Giblin, and J. Sugiyama, Phys. Rev. B **89**, 094406 (2014).
- [16] J. Sugiyama, M. Harada, H. Oki, S. Shiraki, T. Hitosugi, O. Ofer, Z. Salman, Q. Song, D. Wang, H. Saadaoui, G. D. Morris, K. H. Chow, W. A. MacFarlane, and R. Kiefl, J. Phys.: Confer. Series **551**, 012009 (2014).